

necessary to reach a between-sample standard deviation $\leq 0.25\%$ with a probability of 95%. Such biological intrinsic and irreducible variability between coeval individuals, and thus samples, clearly questions the interest for single-cell analyses, more precisely, for coastal marine species, such as *Elphidium*, subject to many environmental changes during their life-time. Indeed, strong variations in salinity or temperature, as well as biogenic fractionation, could influence the isotopic composition of an individual specimen. Results might be less problematic for an average community including several tests. This paper underlines uncertainties linked to specific environments in which selected organisms live, especially for paleoceanographic or paleoclimatic reconstruction purposes where secular oxygen and carbon isotope variations typically range from 0.5 to 1.5‰.

Keywords: stable isotope, foraminifera, ostracod, heterogeneity, single shell analysis

1. INTRODUCTION

Stable oxygen isotope measurements of carbonated fossil shells were the pioneering studies for determining the temperatures of past seawater (Urey, 1947; McCrea, 1950; Epstein et al., 1953). Many carbonate-secreting marine organisms are confined to marine platform settings. Such environments are highly influenced by continental runoff and coastal oceanic currents ultimately affecting, e.g., the depth gradients of temperature and salinity, and pycnocline and nutricline depths. Coccoliths constitute a large fraction of the oceanic nanoplankton since the Early Jurassic but their very small size (a few μm) still makes difficult the isotopic analysis of fossils at the species, or at least at the genus level (but see, e.g., Stoll and Ziveri, 2002; Stoll and Shimizu, 2009; Fink et al., 2010). Foraminifera are also unicellular organisms which size classically ranges from 40 μm up to ~ 1 mm; they appeared during the early Paleozoic but benthic and planktonic forms invaded the deep and surface oceans since the Cretaceous (Roth, 1989). The carbon and oxygen isotope compositions of their shells have been widely used to reconstruct marine paleoproductivity and paleotemperatures. For example, Shackleton (1967; 1986), Shackleton and Opdyke (1973) and Shackleton et al. (1983) revealed the existence of a first-order long-term cooling of Earth's surface since the Paleocene as well as the periodicity of the Quaternary glacial-interglacial stages. Huber et al. (1995; 2002), Schmidt and Mysak (1996) and Jenkyns et al. (2004) showed that the Cretaceous oceans about 100 My ago were much warmer than today, especially at high latitudes in the absence of permanent polar ice caps. The occurrence of foraminifera above and below the thermocline as well as from low to high latitudes led many researchers to use their stable isotope compositions, combined to Mg/Ca ratios, as proxies for both thermal structure of the oceans and volume of freshwater ice stored on the continents (e.g. Billups and Schrag, 2003; Lea et al., 2006).

For these large scales, in space (open ocean) and time (several hundred years resolution), measurements made on several species of the same aliquot seem to reflect the general (regional) conditions, within acceptable uncertainties for natural

environmental changes (van Sebille et al., 2014). The question of robustness and significance of the isotopic analysis is raised for a small amount of foraminifera, taken in specific areas (such as coastal areas) undertaking strong environmental variations.

In the past two decades, increase in the sensitivity of dual-inlet isotope ratio mass spectrometers and their coupling to automated on-line preparation devices allowed the analysis of very small amounts of calcium carbonate, down to the 5–10 μg level. This instrumental improvement opened the field of analysis of single carbonate-secreting unicellular organisms such as foraminifera with weights ranging from a few tenths to hundreds micrograms for most of them. Consequently, many workers established carbon and oxygen isotope seawater curves based on such single shell analysis techniques (e.g. Kelly et al., 1996; Price et al., 1998; Zachos et al., 2007). Nevertheless, inter-individual isotopic variability for both C and O has already been documented (Shuxi and Shackleton, 1990; Billups and Spero, 1995; Saraswati, 2004) and cannot be reduced only to analytical and instrumental accuracy. However, no convincing demonstration was made so far for identifying the environmental (temperature, $\delta^{18}\text{O}$ of water, productivity and $\delta^{13}\text{C}$ of DIC) and biological (physiology and phylogeny) drivers responsible for such isotopic differences between analyzed specimens. The knowledge of the amplitude of the inter-individual oxygen isotope variability is critical considering that most short- and long-term changes in the mean annual or seasonal temperature of surface waters that did not exceed 5°C against up to 15°C for deep waters during the Phanerozoic (e.g. Shackleton, 1986; Zachos et al., 2001; 2003; Pucéat et al., 2003; Joachimski et al., 2009). Indeed, the slope of the oxygen isotope fractionation equation between calcium carbonate and water is slightly higher than 4, hence corresponding to the temperature amplitude recorded by 1‰ change in the $\delta^{18}\text{O}$ value of any aquatic carbonated shell. On the other hand, short-term changes in productivity as well as long-term variations in oxidation or burial of sedimentary organic matter typically produce variations of $\pm 3\%$ in the carbon isotope composition of seawater (Schidlowski, 1987).

Consequently, the aim of this study is to explore the amplitude of both carbon and oxygen isotopic variability as a function of sample size (i.e., number of individual shells pooled in a sample). Selected targets were benthic foraminifera (*Elphidium* and *Ammonia*) and ostracods (*Aurila*) since they have been used for some paleoenvironmental reconstructions of aquatic environments (Holmes, 1996; Bauch et al., 2004). We are conscious that these species are not the most representative of large scale (in space and time) environmental reconstructions in paleoceanography. Although, as they are coastal species, strong environmental parameter changes are expected, and therefore, isotopic measurements performed on individual specimens could reflect strong range of variations.

2. MATERIAL AND METHODS

2.1. SAMPLE ORIGIN

The studied fossil samples come from the Sarmatian (Middle Miocene, 12.8–11.5 Ma) deposits of three boreholes (Perbál-5, Mány-17 and Mány-22) in the Zsámbék Basin, Hungary, which is located in the central part of the Pannonian Basin (Fig. 1 and 2). The lithology of the Sarmatian deposits is heterogeneous: clays, clay marls, calcareous marls, sandstones and limestones. The Sarmatian sequences are underlain by Badenian strata and overlain by Pannonian or Pleistocene sediments.



Figure 1: Geographical location of the studied fossils that were sampled from the Sarmatian (Middle Miocene, 12.8–11.5 Ma) deposits of three boreholes (Perbál-5, Mány-17 and Mány-22) in the Zsámbék Basin, Hungary.

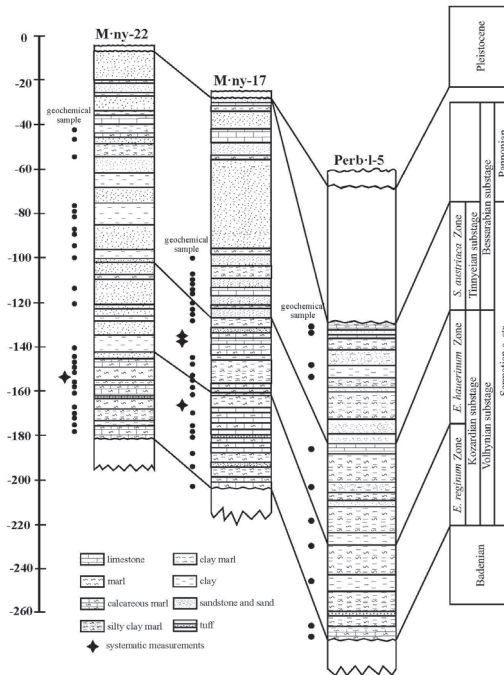


Figure 2: Lithostratigraphic Sarmatian successions in the three boreholes and location of foraminifera and ostracod samples.

For the analyses, very well preserved calcitic shells of foraminifera (*Elphidium aculeatum*, *E. macellum* and *Ammonia beccarii*) and ostracods (*Aurila mehesi* and *A. notata*) were selected (Fig. 3; see Görög (1992) and Tóth (2008) for detailed systematic descriptions of the studied species). The fossil shells are derived from 102 layers of the boreholes (Fig. 2, Appendix A). Additional specimens from four marly beds (Fig. 2, Appendix B) were collected for the systematic isotopic measurements.

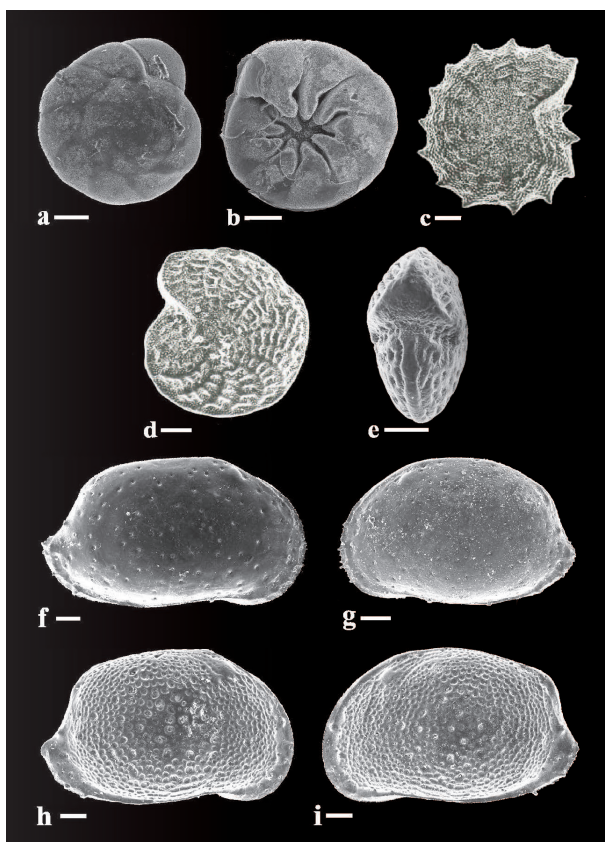


Figure 3: Foraminifera and ostracod species selected for stable carbon and oxygen isotope measurements. Scale bar=100 μm

- (a) *Ammonia beccarii* (Linné). Dorsal side. Mány-22 borehole, depth 45-52.5 m.
- (b) *Ammonia beccarii* (Linné). Ventral side. . Mány-22 borehole, depth 45-52.5 m.
- (c) *Elphidium aculeatum* (d'Orbigny). Side view. Mány-17 borehole, depth 152.8-153 m.
- (d) *Elphidium macellum* (Fichtel & Moll). Side view. Mány-22 borehole, depth 170-173 m.
- (e) *Elphidium macellum* (Fichtel & Moll). Apertural view. Mány-22 borehole, depth 170-173 m.
- (f) *Aurila mehesi* (Zalányi). RV. Mány-17 borehole, depth 168.7-171.2 m.
- (g) *Aurila mehesi* (Zalányi). LV. Mány-17 borehole, depth 168.7-171.2 m.
- (h) *Aurila notata* (Reuss). RV. Mány-22 borehole, depth 45-52.5 m.
- (i) *Aurila notata* (Reuss). LV. Mány-22 borehole, depth 45-52.5 m.

2.2. SAMPLE TREATMENT

For each core sample and both C and O investigations, about 100 g of air-dried sediment was soaked in a dilute solution of hydrogen peroxide and then washed over a column of sieves of diminishing mesh sizes to extract the carbonated shells (foraminifera and ostracods). Then the shells were cleaned three times with deionized water in an ultrasonic bath to remove the sedimentary matrix, and finally hand-picked under a stereomicroscope. In all samples, the calcitic shells of foraminifera and ostracods preserved their original crystal structure as it was evidenced by X-ray diffraction data (Tóth et al., 2010), therefore precluding any diagenetic alteration of the pristine carbon and oxygen isotope compositions of the studied fossils.

2.3. ISOTOPE RATIO MEASUREMENT

Carbon and oxygen isotope ratio measurements have been performed with a MultiPrep system on line with a dual Inlet IsoPrime™ Isotope Ratio Mass Spectrometer (IRMS). The principle of the fully automated device is to react the calcium carbonates with anhydrous phosphoric acid at 90°C to generate CO₂ according to the following acid–base reaction:



Each sample was carefully ground into a powder with grain sizes around 200 µm. Then the sample aliquot (typically 200 – 300 µg) was placed at the bottom of a V shape vial that was then sealed with a rubber septum. The sample vials were then placed in a temperature regulated sample tray heated at 90°C. From this stage all the sample preparation is done automatically. The MultiPrep system is equipped with a double hole needle which allows the acid to be delivered in the vial and also to extract the CO₂ which has been generated during the reaction. First the vial is evacuated through the external needle connected to the MultiPrep vacuum system. Then phosphoric acid is admitted in the vial through the inner needle using the acid pump. At this stage the reaction starts and CO₂ is generated. The reaction time is 20 min and during all this time the needle remains inside the valve. The external cold finger is maintained at -165°C and the valve arrangement allows the CO₂ generated from the reaction to be constantly extracted and trapped in the external cold finger. Once the reaction is completed the external cold finger is heated at -70°C to release the CO₂ without releasing water. The CO₂ pressure is read with a transducer located on the sample side of the IRMS Dual Inlet and from this pressure reading the sample analysis strategy is decided. If the sample is big enough it will be loaded in the dual inlet sample bellow and analyzed. If the sample is too small, it will be trapped in the Dual Inlet cold finger and analyzed.

3. RESULTS

3.1. BACKGROUND INSTRUMENTAL UNCERTAINTY

Determination of the instrumental noise is a prerequisite to any quantification of the carbon and oxygen isotopic variability between biological samples as a function of the number of analyzed individuals per sample. Therefore three sets of measurements have been performed on the international standard NBS-19 and an internal standard (Carrara Marble). Both were routinely measured on a daily basis over 2 months. Instrumental standard deviations associated with $\delta^{18}\text{O}$ and $\delta^{13}\text{C}$ measurements of “large” aliquots ($\sim 300\ \mu\text{g}$) of both NBS-19 and Carrara marble are of 0.062‰ and 0.022‰ (NBS-19, $n=49$) (Table 1; Figure 4), and of 0.069‰ and 0.036‰ (Carrara marble, $n=30$) (Table 2; Figure 5), respectively. These comparable results allow concluding that both calcium carbonate matrices have the same degree of isotopic homogeneity, and that the Carrara marble can be consequently used instead of NBS-19 in order to evaluate the standard deviations associated with measurements of natural samples of varying size.

TABLE 1: Carbon and oxygen isotope compositions of NBS19 aliquots over a period of six months. Sample weights vary from 280 to 390 μg . N.a.: not applicable (in case where only one measurement was performed).

NBS-19-#	$\delta^{13}\text{C}$ ‰ V-PDB	S.D.	$\delta^{18}\text{O}$ ‰ V-PDB	S.D.
NBS19-1	1.93	0.004	-2.33	0.011
NBS19-2	1.96	0.026	-2.16	0.185
NBS19-3	1.96	0.081	-2.16	0.239
NBS19-4	1.94	0.024	-2.26	0.100
NBS19-5	1.94	0.027	-2.15	0.222
NBS19-6	1.96	0.023	-2.23	0.041
NBS19-7	1.92	n.a.	-2.27	n.a.
NBS19-8	1.98	0.042	-2.14	0.092
NBS19-9	1.93	0.016	-2.22	0.058
NBS19-10	1.96	0.017	-2.15	0.094
NBS19-11	1.93	0.007	-2.30	0.027
NBS19-12	1.95	0.022	-2.23	0.050
NBS19-13	1.97	n.a.	-2.17	n.a.
NBS19-14	1.98	0.011	-2.12	0.013
NBS19-15	1.91	0.006	-2.18	0.131
NBS19-16	1.93	n.a.	-2.29	n.a.
NBS19-17	1.98	0.032	-2.12	0.125
NBS19-18	1.96	0.058	-2.22	0.081
NBS19-19	1.94	0.027	-2.17	0.134
NBS19-20	1.93	0.003	-2.33	0.017
NBS19-21	1.96	0.027	-2.15	0.068
NBS19-22	1.96	0.000	-2.12	0.046
NBS19-23	1.94	0.011	-2.24	0.019

Ctnd. **TAB. 1.**

NBS19-24	1.96	0.023	-2.16	0.047
NBS19-25	1.94	0.041	-2.26	0.132
NBS19-26	1.93	0.023	-2.24	0.055
NBS19-27	1.98	0.007	-2.11	0.002
NBS19-28	1.93	0.055	-2.21	0.194
NBS19-29	1.94	0.010	-2.26	0.021
NBS19-30	1.97	0.021	-2.14	0.038
NBS19-31	1.95	0.010	-2.20	0.005
NBS19-32	1.95	0.007	-2.20	0.006
NBS19-33	1.95	n.a.	-2.20	n.a.
NBS19-34	2.00	0.057	-2.31	0.139
NBS19-35	1.90	0.034	-2.08	0.154
NBS19-36	1.97	0.028	-2.21	0.107
NBS19-37	1.95	0.031	-2.22	0.041
NBS19-38	1.98	0.001	-2.16	0.034
NBS19-39	1.97	0.047	-2.15	0.212
NBS19-40	1.96	0.005	-2.20	0.039
NBS19-41	1.90	0.044	-2.28	0.101
NBS19-42	1.95	0.021	-2.20	0.063
NBS19-43	1.95	0.028	-2.20	0.121
NBS19-44	1.95	0.010	-2.20	0.087
NBS19-45	1.97	0.036	-2.25	0.087
NBS19-46	1.96	0.022	-2.16	0.094
NBS19-47	1.93	0.038	-2.17	0.124
NBS19-48	1.98	0.054	-2.11	0.123
NBS19-49	1.92	0.072	-2.30	0.181

TABLE 2: Carbon and oxygen isotope compositions of Carrara marble aliquots over a period of six months. Sample weights vary from 100 to 350 μg .

CM-#	$\delta^{13}\text{C}$ ‰ V-PDB	S.D.	$\delta^{18}\text{O}$ ‰ V-PDB	S.D.
CM1	1.993	0.044	-1.762	0.061
CM2	2.029	0.015	-1.962	0.079
CM3	2.082	0.017	-1.819	0.006
CM4	2.037	0.023	-1.836	0.051
CM5	2.054	0.072	-1.758	0.194
CM6	2.054	0.031	-1.846	0.010
CM7	1.987	0.023	-1.975	0.068
CM8	1.963	0.011	-2.056	0.026
CM9	1.987	0.032	-1.968	0.109
CM10	1.912	0.083	-2.016	0.180
CM12	1.944	0.044	-1.796	0.061
CM13	2.009	0.076	-1.846	0.043
CM14	1.997	0.080	-1.828	0.029
CM15	1.995	0.063	-1.917	0.101
CM16	2.067	0.024	-1.826	0.110
CM18	1.990	0.063	-1.884	0.114
CM20	2.043	0.037	-1.880	0.045

Ctnd. **TAB. 2.**

CM21	1.958	0.061	-1.865	0.088
CM22	2.032	0.030	-1.833	0.020
CM23	2.018	0.032	-1.849	0.052
CM24	2.029	0.052	-1.837	0.058
CM25	2.019	0.026	-1.848	0.085
CM26	2.034	0.030	-1.822	0.022
CM27	2.016	0.026	-1.861	0.021
CM28	2.028	0.056	-1.830	0.088
CM29	2.022	0.019	-1.853	0.053
CM30	2.029	0.024	-1.832	0.066
CM31	2.020	0.022	-1.852	0.044
CM32	2.028	0.025	-1.834	0.033
CM33	2.021	0.010	-1.851	0.027

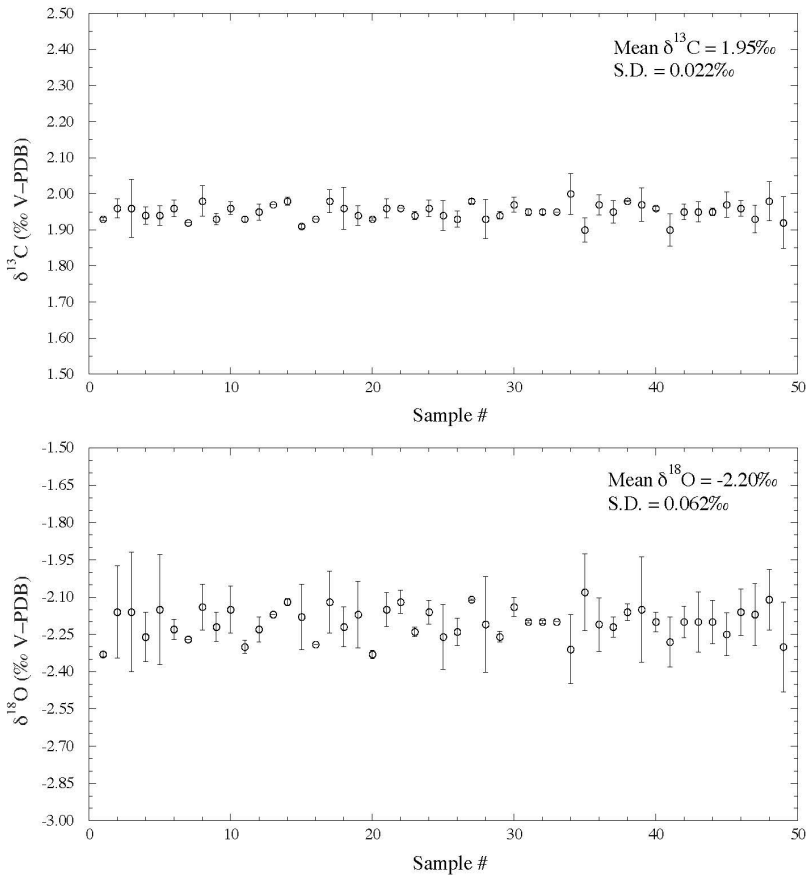


Figure 4: Evolution of $\delta^{13}\text{C}$ and $\delta^{18}\text{O}$ values of NBS 19 reference calcite over a period of six months. Sample sizes vary from 280 to 390 μg .

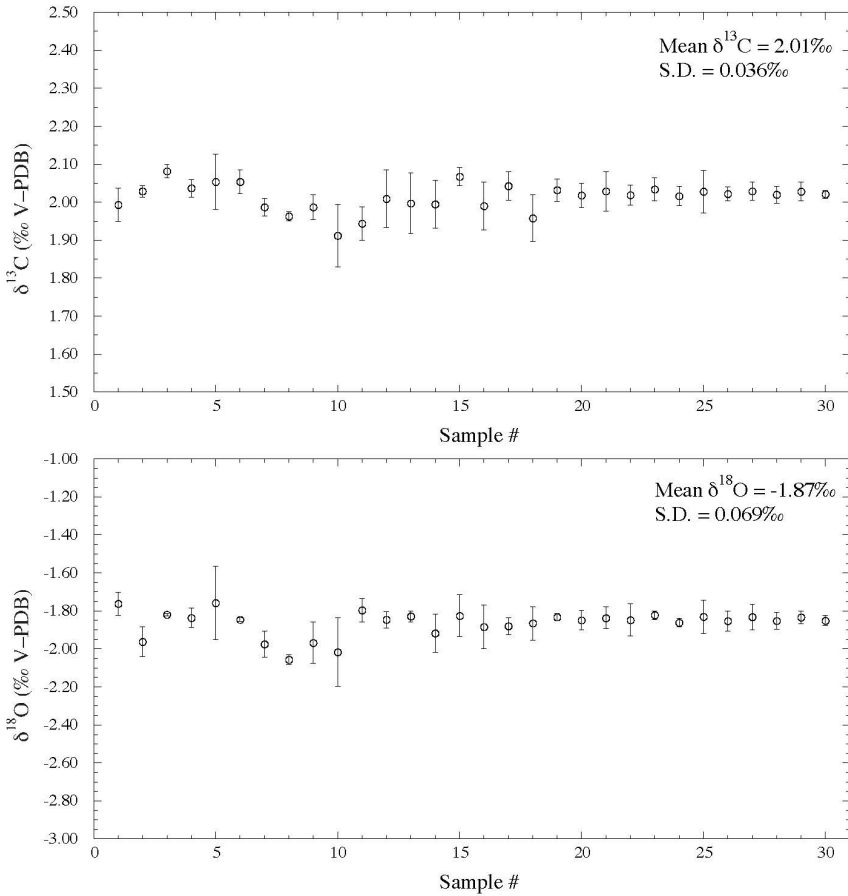
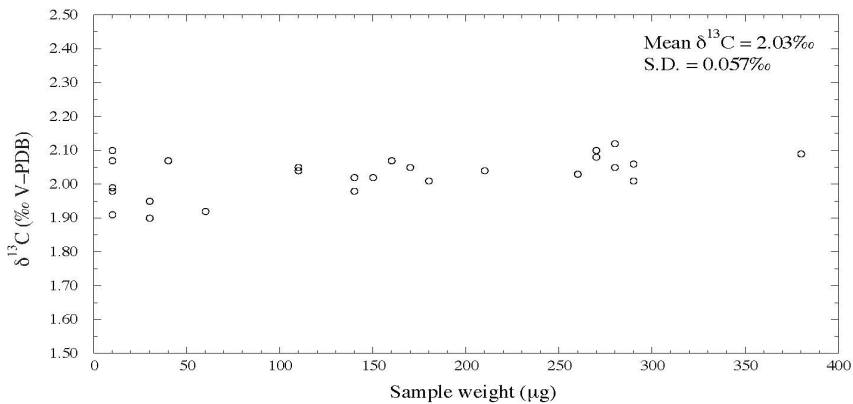


Figure 5: Evolution of $\delta^{13}\text{C}$ and $\delta^{18}\text{O}$ values of Carrara marble over a period of six months. Sample sizes vary from 100 to 350 μg .

Consequently, $\delta^{18}\text{O}$ and $\delta^{13}\text{C}$ standard deviations corresponding to the background instrumental noise have been further estimated for a series of Carrara marble aliquots of varying weight from 10 to 380 μg ; the 29 performed measurements reveal that average instrumental standard deviations associated with $\delta^{18}\text{O}$ and $\delta^{13}\text{C}$ are of 0.133‰ and 0.057‰, respectively (Table 3; Figure 6). It is worth noting here that the average instrumental standard deviations estimated for aliquots ranging from 10 to 60 μg (0.155‰ for $\delta^{18}\text{O}$, and 0.067‰ for $\delta^{13}\text{C}$) were larger than those obtained for aliquots ranging from 110 to 380 μg (0.093‰ for $\delta^{18}\text{O}$ and 0.035‰ for $\delta^{13}\text{C}$), illustrating the expected increase in instrumental uncertainty with decreasing quantity of analyzed material (Fig. 6).

TABLE 3: Carbon and oxygen isotope compositions of Carrara marble aliquots which sample sizes range from 10 to 380 µg.

Sample Name	Weight (µg)	$\delta^{13}\text{C}$ ‰ V-PDB	$\delta^{18}\text{O}$ ‰ V-PDB
CM8	10	1.99	-1.90
CM15	10	2.07	-1.59
CM22	10	2.10	-1.58
CM23	10	1.99	-1.68
CM27	10	1.99	-1.64
CM28	10	1.91	-1.80
CM29	10	1.98	-1.56
CM7	30	1.90	-2.03
CM24	30	1.95	-1.76
CM25	40	2.07	-1.65
CM26	60	1.92	-1.88
CM4	110	2.04	-1.85
CM5	110	2.05	-1.80
CM14	110	2.05	-1.78
CM19	140	2.02	-1.85
CM20	140	1.98	-1.99
CM21	150	2.02	-1.93
CM6	160	2.07	-1.69
CM13	170	2.05	-1.86
CM12	180	2.01	-1.87
CM3	210	2.04	-1.96
CM2	260	2.03	-2.04
CM10	270	2.10	-1.82
CM11	270	2.08	-1.81
CM16	280	2.12	-1.71
CM17	280	2.05	-1.86
CM1	290	2.01	-1.99
CM9	290	2.06	-1.83
CM18	380	2.09	-1.84



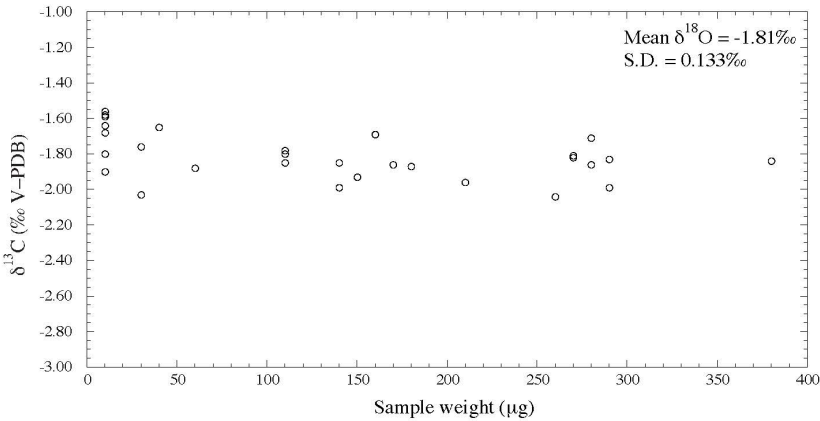


Figure 6: Variations in $\delta^{13}\text{C}$ and $\delta^{18}\text{O}$ values as a function of sample weights (10 to 380 μg) of Carrara marble.

3.2. INTER-INDIVIDUAL BIOLOGICAL VARIABILITY

Taking into account this background instrumental uncertainty, the following hypothesis was tested with natural microfossil samples of foraminifera (*Elphidium*; $n=51$ and *Ammonia*; $n=16$) and ostracods (*Aurila*; $n=34$): for a given sample weight, the between-biological sample isotopic variability should be independent on the number of individuals pooled in each analyzed sample. Table 4 and Figure 7 show that between-biological sample standard deviations related to $\delta^{18}\text{O}$ and $\delta^{13}\text{C}$ average empirical values increase up to 0.7‰ ($\delta^{18}\text{O}$) and 0.85‰ ($\delta^{13}\text{C}$) with the number of individuals decreasing; most values being larger than the background instrumental standard deviations. Data were non-linearly least-square fitted with a power law, assuming that the standard deviation tends towards infinite values when the number of individuals per sample tends towards zero, whilst it should tend towards the background instrumental noise, i.e. the standard deviation defined by either large samples of NBS-19 or Carrara marble, when the number of individuals per sample becomes very large.

TABLE 4: Carbon and oxygen isotope compositions of Sarmatian foraminifera (*Elphidium*, *Ammonia*) and ostracod (*Aurila*) samples. Standard deviations were calculated from two replicates of each sample.

Sample #	Species	Weight (μg)	Individuals (n)	Mean $\delta^{13}\text{C}$ ‰ V-PDB	S.D.	Mean $\delta^{18}\text{O}$ ‰ V-PDB	S.D.
PB-5-1	<i>Elphidium aculeatum</i>	300	10	-1.00	0.078	-1.07	0.018
PB-5-4	<i>Elphidium macellum</i>	300	15	-0.98	0.055	-1.69	0.108
PB-5-5	<i>Elphidium macellum</i>	290	14	0.39	0.252	-1.25	0.147
PB-5-7	<i>Elphidium aculeatum</i>	300	9	0.73	0.111	0.25	0.160

ctnd. **TAB. 4.**

PB-5-8	<i>Elphidium macellum</i>	310	12	0.04	0.102	0.20	0.182
PB-5-17	<i>Elphidium macellum</i>	310	15	0.55	0.004	-0.52	0.150
PB-5-20	<i>Elphidium macellum</i>	300	8	0.77	0.111	-2.93	0.164
PB-5-21	<i>Elphidium macellum</i>	310	5	0.91	0.443	-2.53	0.005
PB-5-23	<i>Elphidium macellum</i>	310	14	1.10	0.069	-2.93	0.217
PB-5-25	<i>Elphidium macellum</i>	310	14	1.29	0.055	-2.35	0.038
PB-5-26	<i>Elphidium macellum</i>	310	6	0.55	0.260	-2.30	0.036
PB-5-28	<i>Elphidium aculeatum</i>	320	13	0.58	0.096	-2.34	0.083
PB-5-29	<i>Elphidium macellum</i>	310	7	1.54	0.040	-2.13	0.081
PB-5-33	<i>Elphidium macellum</i>	300	9	1.50	0.079	-1.68	0.287
PB-5-34	<i>Elphidium aculeatum</i>	310	5	1.80	0.040	-0.45	0.025
PB-5-36	<i>Elphidium macellum</i>	300	12	1.82	0.005	-1.73	0.137
PB-5-38	<i>Elphidium aculeatum</i>	310	16	0.48	0.073	-0.13	0.170
PB-5-46	<i>Elphidium hauerinum</i>	280	41	-0.16	0.021	-0.77	0.061
PB-5-47	<i>Elphidium macellum</i>	310	26	-0.69	n.a.	-1.92	0.021
PB-5-48	<i>Elphidium macellum</i>	280	35	-0.55	0.064	-1.87	0.031
PB-5-50	<i>Elphidium macellum</i>	310	18	-0.62	0.082	-2.58	0.102
PB-5-51	<i>Elphidium macellum</i>	300	25	-0.36	0.107	-1.59	0.197
PB-5-53	<i>Elphidium macellum</i>	300	26	0.13	0.123	-1.35	0.010
PB-5-54	<i>Elphidium macellum</i>	300	24	0.88	0.060	-1.62	0.184
PB-5-57	<i>Elphidium macellum</i>	290	33	-0.20	0.004	-0.53	0.116
M-17-2	<i>Elphidium macellum</i>	310	21	0.75	0.027	-2.47	0.137
M-17-4	<i>Elphidium macellum</i>	310	17	0.59	0.322	-1.00	0.052
M-17-6	<i>Elphidium aculeatum</i>	330	7	1.35	0.140	-1.43	0.125
M-17-8	<i>Elphidium aculeatum</i>	310	10	2.45	0.429	-1.00	0.122

ctnd. **TAB. 4.**

M-17-11	<i>Elphidium macellum</i>	320	18	1.53	0.072	-1.09	0.108
M-17-13	<i>Elphidium aculeatum</i>	330	14	1.13	0.134	-0.59	0.178
M-17-14	<i>Elphidium aculeatum</i>	330	13	0.88	0.043	-0.73	0.394
M-17-16	<i>Elphidium macellum</i>	310	46	-0.08	0.029	-1.09	0.091
M-17-18	<i>Elphidium macellum</i>	310	21	1.38	0.263	-1.52	0.029
M-17-20	<i>Elphidium macellum</i>	310	12	-0.37	0.296	-1.20	0.136
M-17-22	<i>Elphidium macellum</i>	300	14	0.27	0.097	-2.22	0.037
M-17-24	<i>Elphidium macellum</i>	290	16	-0.59	0.027	-1.32	0.042
M-17-25	<i>Elphidium macellum</i>	320	27	-0.09	0.005	-2.24	0.277
M-17-26	<i>Elphidium macellum</i>	320	21	-0.40	0.039	-1.70	0.191
M-17-29	<i>Elphidium macellum</i>	320	10	1.08	0.034	-1.46	0.139
M-17-30	<i>Elphidium macellum</i>	290	27	0.38	0.043	-0.84	0.080
M-17-31	<i>Elphidium aculeatum</i>	300	21	-0.12	0.073	-1.13	0.068
M-17-32	<i>Elphidium macellum</i>	300	21	0.98	0.101	-1.48	0.147
M-17-34	<i>Elphidium macellum</i>	310	17	1.30	0.475	-3.21	0.090
M-17-36	<i>Elphidium macellum</i>	300	8	1.86	0.092	-2.83	0.070
M-17-37	<i>Elphidium macellum</i>	310	14	-0.98	0.145	-1.18	0.032
M-17-38	<i>Elphidium macellum</i>	290	11	1.92	0.006	-1.19	0.124
M-17-40	<i>Elphidium macellum</i>	290	13	0.58	0.210	-2.28	0.423
M-17-42	<i>Elphidium macellum</i>	310	10	1.04	0.316	-2.52	0.055
M-17-44	<i>Elphidium macellum</i>	310	13	1.11	0.229	-2.18	0.066
M-17-46	<i>Elphidium macellum</i>	320	28	0.49	0.348	-1.74	0.689
PB-5-6	<i>Ammonia becarii</i>	240	35	-0.72	0.167	-2.15	0.178
PB-5-11	<i>Ammonia becarii</i>	210	25	-0.09	0.003	-1.08	0.183
PB-5-13	<i>Ammonia becarii</i>	350	14	0.65	0.003	-2.49	0.190

ctnd. **TAB. 4.**

PB-5-16	<i>Ammonia becarii</i>	320	1	0.36	0.099	-2.20	0.293
PB-5-31	<i>Ammonia becarii</i>	310	19	0.91	0.062	-2.90	0.108
PB-5-37	<i>Ammonia becarii</i>	290	25	0.67	0.072	-1.98	0.077
PB-5-42	<i>Ammonia becarii</i>	300	28	-0.13	0.071	-2.77	0.201
PB-5-43	<i>Ammonia becarii</i>	290	36	-0.33	0.084	-2.15	0.081
PB-5-44	<i>Ammonia becarii</i>	300	41	0.93	0.089	-2.05	0.115
PB-5-45	<i>Ammonia becarii</i>	300	44	-0.84	0.100	-1.09	0.051
PB-5-49	<i>Ammonia becarii</i>	310	52	-0.94	0.010	-2.46	0.012
PB-5-55	<i>Ammonia becarii</i>	300	15	1.14	0.085	-2.46	0.037
M-17-7	<i>Ammonia becarii</i>	300	11	1.09	0.034	-2.66	0.169
M-17-10	<i>Ammonia becarii</i>	320	33	0.51	0.118	-0.99	0.003
M-17-12	<i>Ammonia becarii</i>	330	23	0.91	0.046	-2.09	0.534
M-17-21	<i>Ammonia becarii</i>	310	35	0.47	0.271	-1.91	0.040
PB-5-2	<i>Aurila mehesi</i>	300	5	-2.86	0.127	-0.58	0.170
PB-5-3	<i>Aurila notata</i>	300	5	-5.13	0.741	-0.68	0.274
PB-5-9	<i>Aurila notata</i>	280	3	-6.01	0.327	-0.22	0.039
PB-5-10	<i>Aurila notata</i>	310	9	-6.11	0.090	-0.53	0.102
PB-5-12	<i>Aurila notata</i>	300	8	-3.29	0.156	-1.48	0.106
PB-5-15	<i>Aurila notata</i>	300	9	-4.87	0.296	-0.56	0.260
PB-5-18	<i>Aurila mehesi</i>	300	10	-4.24	0.293	-1.14	0.228
PB-5-19	<i>Aurila mehesi</i>	310	8	-2.76	0.323	-2.65	0.306
PB-5-22	<i>Aurila mehesi</i>	320	7	-2.45	0.085	-1.81	0.031
PB-5-24	<i>Aurila mehesi</i>	310	4	-0.50	0.009	-2.23	0.236
PB-5-27	<i>Aurila mehesi</i>	330	6	-2.37	0.388	-2.21	0.174
PB-5-30	<i>Aurila mehesi</i>	300	7	-2.23	0.217	-2.63	0.006

ctnd. **TAB. 4.**

PB-5-32	<i>Aurila mehesi</i>	300	11	-1.93	0.113	-0.89	0.161
PB-5-35	<i>Aurila notata</i>	300	9	-1.79	0.113	-2.58	0.154
PB-5-39	<i>Aurila notata</i>	310	14	-5.21	0.073	-1.44	0.426
PB-5-40	<i>Aurila notata</i>	300	8	-4.36	0.028	-0.70	0.528
PB-5-41	<i>Aurila notata</i>	320	9	-3.84	0.053	-1.42	0.152
PB-5-52	<i>Aurila notata</i>	310	8	-3.57	0.180	-1.52	0.237
PB-5-56	<i>Aurila notata</i>	320	9	-3.39	0.439	-2.44	0.152
M-17-1	<i>Aurila mehesi</i>	290	10	-2.75	0.285	-1.82	0.031
M-17-3	<i>Aurila mehesi</i>	330	8	-2.65	0.082	-2.23	0.220
M-17-5	<i>Aurila mehesi</i>	320	8	-2.96	0.227	-1.27	0.304
M-17-9	<i>Aurila mehesi</i>	300	16	-2.91	0.300	-0.85	0.181
M-17-15	<i>Aurila notata</i>	290	14	-1.71	0.014	-1.79	0.127
M-17-17	<i>Aurila notata</i>	300	4	-4.97	0.447	-0.40	0.009
M-17-19	<i>Aurila notata</i>	300	4	-4.11	0.308	-0.43	0.004
M-17-23	<i>Aurila notata</i>	300	9	-5.03	0.020	-0.57	0.169
M-17-27	<i>Aurila notata</i>	310	8	-3.55	0.356	-1.45	0.083
M-17-28	<i>Aurila notata</i>	300	15	-3.38	0.040	-2.11	0.295
M-17-33	<i>Aurila notata</i>	320	17	-4.20	0.428	-1.81	0.100
M-17-39	<i>Aurila notata</i>	320	6	-3.61	0.221	-2.31	0.314
M-17-41	<i>Aurila notata</i>	330	9	-3.14	0.164	-2.70	0.070
M-17-43	<i>Aurila notata</i>	310	12	-4.20	0.099	-1.25	0.012
M-17-45	<i>Aurila notata</i>	300	10	-3.19	0.849	-2.03	0.203

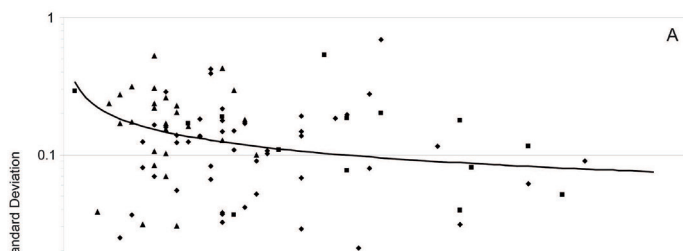


Figure 7: Variations in standard deviations of carbon and oxygen isotope measurements as a function of the number of individuals considering all three genera of foraminifera and ostracods from various levels in Sarmatian boreholes of Hungary (Fig. 2).

The quality of the fit being so weak when considering all three genera from various sample levels simultaneously (due to inter-sample and between-taxon isotopic differences), this approach was restricted to a taxonomically homogeneous pool of *Elphidium* foraminifera extracted from the same, *Elphidium*-rich sample level from the Mány-17 borehole (Fig. 2), from which sub-samples composed of 5, 10, 20, 30 and 40 individual shells (corresponding to samples from 50 to 900 μg) were generated by randomly picking-up the fossils under a stereomicroscope. Single-cell samples were not considered here due to their very small weight (average individual shell weight: $16.5 \pm 3.8 \mu\text{g}$), involving relatively high associated instrumental uncertainty when compared to the 5 to 40-cell samples, and thus biasing upward the estimate of inter-biological sample variability effects. For each sub-sample size, four distinct sub-samples have been made, allowing the computation of a between-biological sample standard deviation (Table 5). Figure 8 shows that this standard deviation increases with the number of individuals decreasing according to the following power laws (including an additive constant which corresponds to the background instrumental standard deviation – a value reached asymptotically when analyzing an “infinite” pool of individuals):

$$\text{SD of } \delta^{18}\text{O} = 0.133 + 34.268 N^{-2.485}, R^2 = 0.83 \text{ (} p = 8.9 \cdot 10^{-2}\text{)}$$

$$\text{SD of } \delta^{13}\text{C} = 0.057 + 2.748 N^{-0.829}, R^2 = 0.92 \text{ (} p = 9.8 \cdot 10^{-3}\text{)},$$

where N is the number of individuals in the sample. According to the prediction confidence interval belts associated to these equations, there is a probability of 95% (lower bound of the 90% C.I. belt) to obtain between-biological sample standard deviations higher than 1.02‰ and 1.45‰ for different $\delta^{18}\text{O}$ and $\delta^{13}\text{C}$ measurements of single specimens of *Elphidium*, respectively. Such predicted inter-individual variability is about one order of magnitude higher than the background instrumental

uncertainty, indicating that a significant amount of variability of eco-physiological origin is added when considering biological organisms such as foraminifera.

TABLE 5: Variations in carbon and oxygen isotope compositions of randomly generated sub-samples of Sarmatian *Elphidium* from a homogeneous pool of *Elphidium macellum* foraminifera extracted from the same level of Mány-17 borehole, Hungary as reported in Figure 2.

Sample #	Individuals (n)	Weight (μg)	$\delta^{13}\text{C}$ ‰ V-PDB	$\delta^{18}\text{O}$ ‰ V-PDB
Elphi M17_1	5	60	0.18	-2.11
Elphi M17_2	5	50	-0.66	-1.52
Elphi M17_3	5	50	-0.55	-1.93
Elphi M17_4	5	60	-1.72	-2.83
Elphi M17_5	10	130	0.33	-1.43
Elphi M17_6	10	140	-0.62	-1.75
Elphi M17_7	10	140	-0.21	-1.63
Elphi M17_8	10	160	-0.26	-1.66
Elphi M17_9	20	380	0.30	-1.69
Elphi M17_10	20	330	0.02	-1.43
Elphi M17_11	20	350	-0.50	-1.68
Elphi M17_12	20	330	-0.15	-1.88
Elphi M17_13	30	570	-0.11	-1.43
Elphi M17_14	30	540	0.27	-1.55
Elphi M17_15	30	610	-0.12	-1.79
Elphi M17_16	30	610	-0.33	-1.61
Elphi M17_17	40	710	-0.26	-1.47
Elphi M17_18	40	850	-0.34	-1.64
Elphi M17_19	40	790	-0.51	-1.74
Elphi M17_20	40	900	-0.13	-1.73

Figure 8: Variations in standard deviations of carbon and oxygen isotope measurements as a function of the number of individuals from the same pool of *Elphidium* foraminifera from the Mány-17 borehole (Fig. 2).

4. DISCUSSION

Isotopic studies of carbonated skeletons cannot escape the question of a possible diagenetic alteration that may potentially modify their pristine compositions. Selected foraminifera and ostracod samples from the Miocene deposits of Hungary have been already evaluated for their state of preservation as attested by the quality of their ultrastructure imaged by SEM techniques (Tóth et al., 2010). However, no definitive criterion is available in order to discard unambiguously alteration processes responsible for sizable changes in the post-depositional compositions of carbonated fossils. Nevertheless, on the basis of mass balance considerations, one can expect two isotopic patterns of water–mineral interactions that could operate within sedimentary deposits. The first one is the production of homogenized isotopic compositions of fossils in response to large volumes of aqueous fluids interacting with the hosting sediment; the second one, driven by low water–mineral ratios, should produce isotopic heterogeneities without any relation to the sample size (i.e., number of sampled individuals). These two scenarios do not match the observed distribution of isotopic compositions in studied foraminifera and ostracod shells.

Carbon and oxygen isotope compositions of the studied carbonated fossil shells show unambiguously that empirical between-biological sample variability associated with $\delta^{18}\text{O}$ and $\delta^{13}\text{C}$ largely exceeds the background instrumental uncertainty and clearly relates to inter-individual variability (Fig. 7 and 8). This result clearly impacts interpretation of variations in both $\delta^{18}\text{O}$ and $\delta^{13}\text{C}$ values of marine carbonated microfossils as indicators of change in ambient seawater temperature and productivity.

Indeed, in order to be able to detect subtle variations in seawater temperature based on $\delta^{18}\text{O}$ values, a minimum of 35 pooled specimens of *Elphidium* is necessary to reach a between-sample standard deviation $\leq 0.25\text{‰}$ with a probability of 95%, corresponding to an estimated temperature uncertainty $\leq \pm 1^\circ\text{C}$ at a 95% confidence level (Fig. 8). The analysis of less than 3 pooled individual shells returns standard deviation values $\geq 0.25\text{‰}$ in more than 95% of the sample cases, a value exceeding 1‰ (corresponding to an actual seawater estimated temperature uncertainty of at least $\pm 4^\circ\text{C}$ at a 95% confidence level) when a single specimen of *Elphidium* is analyzed. In such cases of large uncertainty, the detection of thermal events such as changes in oceanic circulation or climatic events recorded by coastal waters (whose amplitudes rarely exceed 5°C as documented since the Mesozoic; Shackleton, 1986; Norris and Röhl, 1999; Lécuyer et al., 2003; Pucéat et al., 2003; Joachimski et al., 2009) obviously becomes problematic, if not impossible. The oxygen isotope composition of benthic foraminifera such as *Elphidium* has been also extensively used as a proxy of variations in the $\delta^{18}\text{O}$ of seawater as a consequence of changes in the continental ice volume. Once again, this threshold of $\sim 1\text{‰}$ associated with the analysis of a single foraminifera shell constitutes a “biological isotopic noise” in the same order of magnitude as the variation in the $\delta^{18}\text{O}$ of the oceans resulting from ice cap growth during a glacial stage or a complete melting of existing ice caps during

a greenhouse interlude (Shackleton and Kennett, 1975; Billups and Schrag, 2003; Pekar and DeConto, 2006). Again, these results challenge the interpretation of the $\delta^{18}\text{O}$ signal for coastal benthic foraminifera only. For the open ocean record, including benthic and planktonic isotopic compositions on a regional interval, quantitative estimations based on several specimens seem to stay valid, taking into account local perturbations such as current strength or origin (Van Sebille et al., 2015). In addition to this study, the same approach needs to be performed on individual benthic or planktonic specimen taken in large scale areas, to investigate open-ocean parameter reconstructions. Deeper studies could also test differences observed at several depths in the water column, taking into account different sizes within a single foraminifera species.

Concerning carbon isotope measurements, a minimum of 15 and 44 *Elphidium* individuals is required in order to reach between-sample standard deviations $\leq 0.5\%$ and $\leq 0.25\%$, respectively (Fig. 8). The carbon isotope analysis of a single specimen generates a standard deviation $\geq 1.45\%$ in 95% of the sample cases; such threshold is comparable to secular changes in the $\delta^{13}\text{C}$ values recorded in the marine carbonate deposits which are interpreted either as variations in the primary production at time scales of about 50,000 yr, or variations in the burial or oxidation rates of sedimentary organic matter at time scales of about 1 Myr (e.g. Magaritz et al., 1992; Kump and Arthur, 1999). However, this between-sample standard deviation predicted for a single specimen analysis in a homogeneous taxonomical and environmental/climatic context is significantly lower than some spectacular carbon isotope excursions recorded in sediments and which were interpreted as related to extreme events such as food chain rupture, volcanic paroxysm and large methane release by clathrates (e.g. Röhl et al., 2000; Pálffy et al., 2001; Hesselbo et al., 2002).

Contrasting with the two relations inferred for $\delta^{18}\text{O}$ and $\delta^{13}\text{C}$, it is worth noting that the average observed values of inter-biological sample standard deviation in the 5–40 specimens and 50–900 μg sample weight ranges are slightly higher for $\delta^{13}\text{C}$ than for $\delta^{18}\text{O}$ measurements. Actually, based on the instrumental standard deviations as evidenced above, one should expect the reverse situation if such inter-biological sample standard deviations were the consequence of an instrumental mass fractionation (the average instrumental error is ~ 2.3 times larger for $\delta^{18}\text{O}$ than for $\delta^{13}\text{C}$ based on 29 Carrara marble aliquots). Indeed, such result clearly points to the fact that the inter-biological sample variability evidenced here does originate in an inter-individual natural heterogeneity (i.e., biological variability) rather than in an instrumental fractionation spurious analytical effect. This result makes sense with regard to the specific environmental life style of *Elphidium*, a coastal species for which strong natural variations in salinity and temperature could be expected.

Inter-individual $\delta^{18}\text{O}$ and $\delta^{13}\text{C}$ variations as evidenced here between specimens from the same foraminifera genus and fossil level are most likely resulting from eco-physiological intrinsic differences in metabolism (e.g., individual position within the autotrophy-heterotrophy gradient) and environmental conditions (e.g., depth-related changes in temperature and luminosity, and composition of dissolved inorganic carbon). In addition, such irreducible biological variability could be strongly, but

artefactually enhanced by cryptic biological speciation events as increasingly evidenced in marine, planktic as well as benthic organisms (Knowlton, 1993; de Vargas et al., 1999, 2004; Irigoien et al., 2004; Chen and Hare, 2008; Darling and Wade, 2008). An efficient way to further exploring such possibility should be to independently perform the kind of analysis leading to Figure 8 on distinct morphological species showing contrasted cryptic diversity contexts (the higher the cryptic diversity, the steeper the decreasing slope of the number of individuals vs. between-sample standard deviation relation). The ongoing effort in developing morphometrical recognition models of cryptic species (e.g., Morard et al. 2009) should allow solving this problem in the future. Future studies could also investigate open ocean foraminifera species, benthic or planktonic, usually used for large-scale (in both space and time) paleoceanographic reconstructions.

5. CONCLUSION

We have shown in this study that recent automated systems designed for the analyses of $\delta^{13}\text{C}$ and $\delta^{18}\text{O}$ from carbonate samples are capable of measuring reliably small quantities of pure calcite down to 5–10 μg with instrumental standard deviations close to 0.1‰. Such analytical accuracy opens up possibilities for the analysis of small microfossils like foraminifera, especially for paleoclimate reconstruction purposes. Nevertheless, data generated from small numbers of specimens (e.g., carbonated shells from single-cell organisms) have to be considered with great caution. Indeed, our results show a general trend to increase the between-biological sample standard deviation for both ^{13}C and ^{18}O measurements when decreasing the number of specimen analysed. Based on a systematic study performed on a homogeneous pool of *Elphidium* coastal benthic foraminifera, we estimate that there is a probability of 95% to obtain between-biological sample standard deviations higher than 1.02‰ and 1.45‰ for $\delta^{18}\text{O}$ and $\delta^{13}\text{C}$ measurements of various single shells, respectively.

Such biological intrinsic and irreducible variability observed between coeval samples clearly questions the interest for single-cell analyses for environments undertaking rapid and strong variations in their physical parameters, such as salinity and temperature. For this specific example, paleotemperature estimates should not be done on single foraminifera $\delta^{18}\text{O}$ measurements.

REFERENCES

1. Bauch H.A., Erlenkeuser H., Bauch D., Mueller-Lupp T., Taldenkova E., 2004. Stable oxygen and carbon isotopes in modern benthic foraminifera from the Laptev Sea shelf: implications for reconstructing proglacial and profluvial environments in the Arctic. *Mar. Micropal.* 5, 285–300.

2. Billups K., Schrag D.P., 2003. Paleotemperatures and ice volume of the past 27 Myr revisited with paired Mg/Ca and $^{18}\text{O}/^{16}\text{O}$ measurements on benthic foraminifera. *Paleoceanography* 17(1), 1003, doi: 10.1029/2000PA000567.
3. Billups K., Spero H.J., 1995. Relationship between shell size, thickness and stable isotopes in individual planktonic foraminifera from two equatorial Atlantic cores. *J. Foram. Res.* 25, 24–37.
4. Chen G., Hare M.P., 2008. Cryptic ecological diversification of a planktonic estuarine copepod, *Acartia tonsa*. *Molecul. Ecol.* 17, 1451–1468.
5. Darling K.F., Wade C.M., 2008. The genetic diversity of planktic foraminifera and the global distribution of ribosomal RNA genotypes. *Mar. Micropal.* 67, 216–238.
6. Epstein S., Buchsbaum R., Lowenstam H.A., Urey, H.C., 1953. Revised carbonate–water isotopic temperature scale. *Geol. Soc. Am. Bull.* 64, 1315–1326.
7. Fink C., Baumann K.-H., Groeneveld J., Steinke S., 2010. Strontium/Calcium ratio, carbon and oxygen stable isotopes in coccolith carbonate from different grain-size fractions in South Atlantic surface sediments. *Geobios* 43, 151–164.
8. Görög A., 1992. Sarmatian foraminifera of the Zsámbék Basin, Hungary. *Annales Universitatis Scientiarum Budapestinensis, Sectio Geologica* 29, 31–153.
9. Hesselbo S.P., Robinson S.A., Surlyk F., Piasecki S., 2002. Terrestrial and marine extinction at the Triassic-Jurassic boundary synchronized with major carbon-cycle perturbation: A link to initiation of massive volcanism? *Geology* 30, 251–254.
10. Holmes J.A., 1996. Trace-element and stable-isotope geochemistry of non-marine ostracod shells in Quaternary palaeoenvironmental reconstruction. *J. Paleolimnol.* 15, 223–235.
11. Huber B.T., Norris R.D., Macleod K.G., 2002. Deep-sea paleotemperature record of extreme warmth during the Cretaceous. *Geology* 30, 123–126.
12. Huber B.T., Hodell D.A., Hamilton C.P., 1995. Mid- to Late Cretaceous climate of the southern high latitudes: stable isotopic evidence for minimal equator-to-pole thermal gradients. *Geol. Soc. Am. Bull.* 107, 1164–1191.
13. Irigoien X., Huisman J., Harris R.P., 2004. Global biodiversity patterns of marine phytoplankton and zooplankton. *Nature* 429, 863–867.
14. Jenkyns H.C., Forster A., Schouten S., Damsté J.S.S., 2004. High temperatures in the Late Cretaceous Arctic Ocean. *Nature* 432, 888–892.
15. Joachimski M.M., Breisig S., Buggisch W., Talent J.A., Mawson R., Gereke M., Morrow J.M., Day J., Weddige K., 2009. Devonian climate and reef evolution: insights from oxygen isotopes in apatite. *Earth. Planet. Sci. Lett.* 284, 599–609.
16. Kelly D.C., Bralower T.J., Zachos J.C., Silva I.P., Thomas E., 1996. Rapid diversification of planktonic foraminifera in the tropical Pacific (ODP site 865) during the Late Paleocene thermal maximum. *Geology* 24, 423–4126.
17. Knowlton N., 1993. Sibling species in the sea. *Ann. Rev. Ecol. Syst.* 24, 189–216.
18. Kump L.R., Arthur M.A., 1999. Interpreting carbon-isotope excursions: carbonates and organic matter. *Chem. Geol.* 161, 181–198.
19. Lea D.W., Pak D.K., Belanger C.L., Spero H.J., Hall M.A., Shackleton N.J., 2006. Paleoclimate history of Galapagos surface waters over the last 135,000 yr. *Quat. Sci. Rev.* 25, 1152–1167.
20. Lécuyer C., Picard S., Garcia J.-P., Sheppard S.M.F., Grandjean P., Dromart G., 2003. Thermal evolution of Tethyan surface waters during the Middle-Late Jurassic: Evidence from $\delta^{18}\text{O}$ values of marine fish teeth. *Paleoceanography* 18 (3), 1076, doi:10.1029/2002PA000863.

21. Magaritz M., Krishnamurthy R.V., Holser W.T., 1992. Parallel trends in organic and inorganic carbon isotopes across the Permian/Triassic boundary. *Am. J. Sci.* 292, 727–739.
22. McCrea J.M., 1950. On the isotopic chemistry of carbonates and a paleotemperature scale. *J. Chem. Phys.* 18, 849–857.
23. Morard R., Quillévéré F., Escarguel G., Ujiie Y., de Garidel-Thoron T., Norris R.D., de Vargas C. 2009. Morphological recognition of cryptic species in the planktonic foraminifer *Orbulina universa*. *Mar. Micropal.* 71, 148–165.
24. Norris R.D., Röhl U., 1999. Carbon cycling and chronology of climate warming during the Palaeocene/Eocene transition, *Nature* 401, 775–778.
25. Pálffy J., Demény A., Haas J., Hetényi M., Orchard M., Veto I., 2001. Carbon isotope anomaly and other geochemical changes at the Triassic-Jurassic boundary from a marine section in Hungary. *Geology* 29, 1047–1050.
26. Pekar S.F., DeConto R.M., 2006. High-resolution ice-volume estimates for the early Miocene: Evidence for a dynamic ice sheet in Antarctica. *Palaeogeogr. Palaeoclimatol. Palaeoecol.* 231, 101–109.
27. Price G.D., Sellwood B.W., Corfield R.M., Clarke L., Cartlidge J.E., 1998. Isotopic evidence for palaeotemperatures and depth stratification of Middle Cretaceous planktonic foraminifera from the Pacific Ocean. *Geol. Mag.* 135, 183–191.
28. Pucéat E., Lécuyer C., Sheppard S.M.F., Dromart G., Reboulet S., Grandjean P., 2003. Thermal evolution of Cretaceous Tethyan marine waters inferred from oxygen isotope composition of fish tooth enamels. *Paleoceanography* 18 (2), 1029, doi:10.1029/2002PA000823.
29. Röhl U., Bralower T.J., Norris R.D., Wefer G., 2000. New chronology for the late Paleocene thermal maximum and its environmental implications. *Geology* 28, 927–930.
30. Roth P.H., 1989. Ocean circulation and calcareous nannoplankton evolution during the Jurassic and Cretaceous. *Palaeogeogr. Palaeoclimatol. Palaeoecol.* 74, 111–126.
31. Saraswati P.K., 2004. Ontogenetic isotopic variation in foraminifera – Implications for palaeo prox. *Current Science* 86, 858–860.
32. Schidlowski M., 1987. Application of stable isotopes to early biochemical evolution on Earth. *Annu. Rev. Earth. Planet. Sci.* 15: 47–72.
33. Schmidt G.A., Mysak L.A., 1996. Can increased poleward oceanic heat flux explain the warm Cretaceous climate? *Paleoceanography* 11, 579–593.
34. Shackleton N.J., Opdyke N.D., 1973. Oxygen isotope and paleomagnetic stratigraphy of equatorial Pacific core V28-2389: oxygen isotopes temperatures and ice volumes on a 10^5 and 10^6 year scale. *Quat. Res.* 3, 39–55.
35. Shackleton N.J., 1967. Oxygen isotope analyses and Pleistocene temperatures reassessed. *Nature* 215, 15–17.
36. Shackleton N.J., 1986. Paleogene stable isotope events. *Palaeogeogr. Palaeoclimatol. Palaeoecol.* 57, 91–102.
37. Shackleton N.J., Imbrie J, Hall M.A., 1983. Oxygen and carbon isotope record of East Pacific core V19-30: Implications for the formation of deep water in the late Pleistocene North Atlantic. *Earth Planet. Sci. Lett.* 65, 233–244.
38. Shackleton N.J., 1986. Paleogene stable isotope events. *Palaeogeogr. Palaeoclimatol. Palaeoecol.* 57, 91–102.
39. Shackleton N.J., Kennett J.P., 1975. Paleotemperature history of the Cenozoic and initiation of Antarctic glaciation: oxygen and carbon isotopic analyses in DSDP Sites 277, 279, and 281. *Init. Rep. Deep Sea Drill. Proj.* 29, 743–755.

40. Shuxi C., Shackleton N.L., 1990. New technique for study on isotopic fractionation between sea water and foraminiferal growing processes. *Chin. J. Ocean. Limnol.* 8, 299–305.
41. Stoll H.M., Shimizu N., 2009. Micropicking of nannofossils in preparation for analysis by secondary ion mass spectrometry. *Nature Protocol* 4, 1038–1043.
42. Stoll H.M., Ziveri P., 2002. Separation of monospecific and restricted coccolith assemblages from sediments using differential settling velocity. *Mar. Micropal.* 46, 209–221.
43. Tóth E., 2008. Sarmatian (Middle Miocene) ostracod fauna from the Zsámbék Basin, Hungary. *Geol. Pann.* 36, 101–51.
44. Tóth E., Görög A., Lécuyer C., Moissette P., Balter V., Monostori M., 2010. Palaeoenvironmental reconstruction of the Sarmatian (Middle Miocene) Central Paratethys based on palaeontological and geochemical analyses of foraminifera, ostracods, gastropods and rodents. *Geol. Mag.* 147, 299–314.
45. Urey H.C., 1947. The thermodynamic properties of isotopic substances. *J. Chem. Soc. London* 1947, 562–587.
46. Van Sebille E., Scussolini P., Durgadoo J.V., Peeters F.J.C., Biastoch A., Weijer W., Turney C., Paris C.B. and Zahn R., 2014. Ocean currents generate large footprints in marine palaeoclimate proxies. *Nature Com.*, doi: 10.1038/ncomms7521.
47. Vargas (de) C., Norris R., Zaninetti L., Gibb S.W., Pawlowski J., 1999. Molecular evidence of cryptic speciation in planktonic foraminifers and their relation to oceanic provinces. *Proc. Nat. Acad. Sci. U.S.* 96, 2864–2868.
48. Vargas (de) C., Sáez A.G., Medlin L.K., Thierstein H.R., 2004. Superspecies in the calcareous plankton. In: Thierstein, H.R., Young, J. (eds.), *Coccolithophores – from Molecular Processes to Global Impact*. Springer-Verlag, Heidelberg, Germany, pp. 271–298.
49. Zachos J.C., Bohaty S.M., John C.M., McCarren H., Kelly D.C., Nielsen T., 2007. The Palaeocene–Eocene carbon isotope excursion: constraints from individual shell planktonic foraminifer records. *Phil. Trans. R. Soc.* 365, 1829–1842.
50. Zachos J.C., Pagani M., Sloan L., Thomas E., Billups K. 2001. Trends, rhythms, and aberrations in global climate 65 Ma to Present. *Science* 292, 686–693.
51. Zachos J.C., Wara M.W., Bohaty S.M., Delaney M.L., Rose-Pettrizzo M., Brill A., Bralower T.J., Premoli-Silva I., 2003. A transient rise in tropical sea surface temperature during the Paleocene-Eocene Thermal Maximum. *Science* 302, 1551–1554.